Alzheimer's Research & Therapy

RESEARCH

Open Access

The relationship between amyloid-β peptide spectrum and the spastic paraparesis phenotype in autosomal dominant Alzheimer's disease

Katarzyna Marta Zoltowska[1,2†], Julia Bandera[1,2†], Mohamed Belal Hamed[1,2,3], Thomas Enzlein[4], Carsten Hopf[4], Natalie S. Ryan[5,6] and Lucía Chávez-Gutiérrez[1,2*]

Abstract

Background More than 300 mutations in presenilin 1 (PSEN1) lead to autosomal dominant Alzheimer's disease (ADAD). PSEN1, as the catalytic subunit of γ-secretase, generates amyloid-β (Aβ) peptides through a sequential proteolysis of the amyloid precursor protein (APP). While ADAD typically presents with progressive cognitive decline, ~ 25% of *PSEN1* mutation carriers develop spastic paraparesis (SP), a debilitating motor condition. The molecular basis of this phenotypic heterogeneity remains unknown. This study examines Aβ profiles generated by PSEN1 variants associated with different clinical presentations with the aim of exploring potential associations between different Aβ profiles and clinical heterogeneity.

Methods We analysed reported Aβ peptide profiles generated in vitro by 160 PSEN1 variants, categorized by their associated AD or AD + SP phenotype. We employed an integrated analytical approach combining univariate comparisons of Aβ profiles with machine learning classification.

Results AD + SP-linked mutations showed significantly higher Aβ43 levels and more severe impairments in γ-secretase processivity compared to pure dementia associated variants. Machine learning consistently identified Aβ43 as the most important feature allowing for the phenotypic classification. Unlike processivity impairments, total Aβ production was comparable between groups, suggesting specific rather than global alterations in γ-secretase function.

Conclusions Our analysis reveals a robust association between elevated Aβ43 levels and SP development in *PSEN1* mutation carriers. While this correlation does not establish causation, the distinct impact of SP-associated mutations on γ-secretase function, resulting in elevated Aβ43 production, suggests that mutation-specific mechanisms may underlie clinical heterogeneity in ADAD, with potential implications for biomarker and translational research.

†Katarzyna Marta Zoltowska and Julia Bandera contributed equally to this work.

*Correspondence:
Lucía Chávez-Gutiérrez
Lucia.ChavezGutierrez@kuleuven.be

Full list of author information is available at the end of the article

Keywords Autosomal dominant Alzheimer's disease, Spastic paraparesis, Presenilin 1, Amyloid beta, Motor impairments, Spasticity

Background

Early-onset, autosomal dominant Alzheimer's disease (ADAD) is a progressive neurodegenerative disorder that typically manifests before the age of 65 [1, 2].Mutations in the presenilin 1 (*PSEN1*) gene are the predominant cause of this condition. In addition, mutations in *PSEN2* and amyloid precursor protein (*APP*) genes, including *APP* duplications, can cause early-onset AD, though these are typically associated with a later clinical onset.

PSEN1 is the catalytic subunit of the γ-secretase complex, an intramembrane protease that sequentially cleaves numerous type I or type III membrane proteins within their transmembrane domains, thereby regulating various physiological processes. The sequential proteolysis of APP has emerged as particularly significant in ADAD pathogenesis. In this process, γ-secretase/PSEN1 yields a spectrum of amyloid beta (Aβ) peptides through sequential cleavage events, where efficient processing generates shorter Aβ peptides [3]. The tight link between this process and ADAD symptom onset and progression has made it a central focus of investigations [4–6]. Notably, pathogenic PSEN1 or PSEN2 variants impair the processive proteolysis of APP/Aβ (γ-secretase processivity), and thereby enhance the generation of longer Aβ peptides, particularly Aβ42 and Aβ43 [7–9]. These longer peptides show increased propensity for aggregation, which promotes their accumulation in the brains of mutation carriers. To date, more than 300 mutations in PSEN1 have been linked to ADAD (Alzforum database).

While classically associated with dementia and cognitive decline, ADAD-linked PSEN1 variants have a heterogenous presentation [2, 10, 11]. In ~ 25% of cases, carriers experience motor symptoms, including spastic paraparesis (SP) and upper limb pyramidal signs. SP, a neurological condition characterized by progressive stiffness (spasticity) without weakness in the lower limbs, represents an atypical presentation in ADAD that can occur alongside or even precede the typical cognitive symptoms. Some case studies highlight a spectrum of motor deficits, including SP, as a primary reason for referral to clinics [12, 13]. However, the SP phenotype typically presents later in the disease course and is predominantly associated with PSEN1 variants [2]. Despite its clinical significance and unique association with PSEN1 mutations, the molecular mechanisms driving SP development remain elusive. The observed (SP) phenotype could result from either altered Aβ metabolism or impairments in Aβ-independent roles of γ-secretase/PSEN1.

Recent in vitro studies, including ours, have provided key insights into the associations between mutation-driven alterations in γ-secretase processivity along APP/Aβ and ADAD development. These investigations established linear relationships between mutation-induced shifts in Aβ profiles generated by cell lines expressing pathogenic *PSEN1*, *PSEN2* and *APP* variants – assessed by the Aβ37 + 38 + 40/42 + 43 ratio – and the age at dementia symptom onset (AAO) [5, 6, 14]. Furthermore, Schultz et al. [6] show that alterations in Aβ profiles strongly associate with measures of cognitive decline and core biomarker data in a study of 161 ADAD-linked PSEN1 variants. Complementing these findings, Liu et al. [4] pointed at the Aβ37/42 ratio as a potential biomarker that differentiates pathological states across multiple contexts: 131 PSEN1 variants (in vitro), as well as brain tissue and cerebrospinal fluid from controls, ADAD and sporadic AD (SAD) affected individuals [4]. These studies not only provide molecular insights into ADAD pathogenesis and dementia onset, but also serve as extensive resources for investigating potential associations between mutation-driven alterations in Aβ production and additional phenotypes in mutation carriers. In particular, exploring possible relationships between ADAD-linked Aβ profiles and motor symptom (SP) development could yield insights that inform future therapeutic strategies targeting these phenotypes.

To investigate the relationships between Aβ profiles and clinical disease presentation (either pure dementia (AD) or AD with SP phenotype (AD + SP)) in *PSEN1* mutation carriers, we integrated and harmonised data from Petit et al. [5], Liu et al. [4] and Schultz et al. [6]. We analysed various Aβ measures that reflect γ-secretase (dys)function between the two phenotypes, and applied machine learning to identify potential Aβ biochemical features associated with SP development. Our analyses reveal that among the measured Aβs, Aβ43 shows the most significant correlation with SP occurrence.

Methods

Datasets used in the analysis

Aβ profiles generated in vitro by cell lines expressing WT or mutant PSEN1s were extracted from the Petit et al. [5], Liu et al. [4] and Schultz et al. [6] which report values for Aβ peptides (37, 38, 39, 40, 42 and 43) produced by 36 PSEN1 variants expressed in *psen1/psen2* deficient mouse embryonic fibroblasts (MEF), 131 and 162 PSEN1 variants expressed in human embryonic kidney (HEK) 293 PSEN1 knock-out cells, [4–6]. In all studies Aβ peptides were measured by MSD-ELISA, using synthetic

Aβ peptides as calibrators. The consistent use of MSD-ELISA methodology across all three datasets facilitated direct comparison and integration through normalization to wild-type PSEN1. To integrate the datasets a normalization step was included, which used the PSEN1 wild type (WT) data as a reference (additional file 1). For the mutations that were analysed in more than one study, the averages were calculated and used in the downstream analysis. Mutations reported not to lead to the reduction in the γ-secretase processivity (A164V, T147P, V82L, E69D, D40del, V94M), and hence likely non-pathogenic, were removed from the analysis to focus on variants with pathogenic biochemical signatures. In addition, mutations reported to lead to profound decrease in γ-secretase activity (R278I, C410Y, P433S) were removed from the analysis because these variants represent a distinct mechanistic class with near-complete loss of enzyme function and produce Aβ profiles enriched in Aβ43, and potentially longer peptides, which would confound comparisons of processivity and product-line preference among pathogenic variants [5, 15]. As controls, to establish the baseline for normal γ-secretase function, Aβ profiles generated by WT PSEN1 and two non-pathogenic variants R35Q and E318G were used.

Groups analysed and statistical analysis

The phenotypic annotation was done using Alzforum data, and "spastic" as a keyword. Several entries were curated based on published literature: SP phenotypes were not annotated in Alzforum but reported in literature for F386S [16], I213F, [17], Y256S [18], M233V [19] and S290C PSEN1 variants [20]. Then, PSEN1 mutations were classified into two groups: those presenting with pure dementia (AD, 118 variants) phenotype and those associated with spastic paraparesis (AD + SP, 39 variants). Amyloid profiles were converted to relative values, i.e. % of a particular Aβ peptide out of the total pool of the Aβ generated (defined as a sum of measured secreted Aβ peptides (37, 38, 40, 42 and 43). In addition, respective Aβ ratios, reporting on product-line preference and overall processivity, were calculated, as described in the results section. Wilcoxon Signed Rank Test was applied for the statistical comparison of the two groups, as the data did not present normal distribution, as determined with Shapiro–Wilk's normality test. $P < 0.05$ was considered as a pre-determined threshold for statistical significance. Principal component analysis (PCA) was applied for the dimensionality reduction on the relative Aβ profile data (Aβ37, Aβ38, Aβ40, Aβ42, and Aβ43 expressed as percentages of total Aβ) from all analysed PSEN1 variants (118 AD and 39 AD + SP variants). To evaluate whether the relationship between processivity and product-line preference of γ-secretase differed between disease groups, we applied analysis of covariance (ANCOVA). Initially, a linear regression model including the interaction term between processivity and disease gruop (AD vs. AD + SP) was fitted to test for differences in slopes. Since the interaction term was not significant, indicating parallel slopes, a reduced model without the interaction term (parallel slopes model) was used to assess differences in intercepts between the two disease groups. 95% confidence intervals were calculated for both slopes and intercepts. The analysis was performed using R version 4.3.2. and the following packages: PCAtools, ggplot2, ggfortify, ggpubr and RColorBrewer, and respective dependencies.

Supervised machine learning

The machine learning analyses were performed using Python 3.10.12, and matplotlib, pandas, numpy, imblearn, scikit-learn and seaborn libraries. Due to the compositional nature of the data, a Centered Log-Ratio (CLR) transformation was applied to create values suitable for machine learning analysis while preserving the relationships between features. The integrated datasets from Liu et al. and Petit et al. were used as the training set, while the Schultz et al. dataset served as an independent test set. Features consisted of five Aβ peptide levels (Aβ37, Aβ38, Aβ40, Aβ42, and Aβ43) expressed as percentages of total measured Aβ after CLR transformation. We addressed class imbalance using two distinct approaches. In the first approach, we applied the Synthetic Minority Over-sampling TEchnique (SMOTE) [21], which selects minority class samples (AD + SP) and their nearest neighbours to generate synthetic data instances along the line segments joining these points. This effectively increased the number of SP + AD samples, helping to balance the dataset and improve the performance of the classification models. Class imbalance was also accounted for during performance evaluation using balanced accuracy, weighted recall, weighted precision, and weighted F1 scores. In the second approach, we analysed the CLR-transformed data without oversampling, instead accounting for class imbalance directly during model training (where supported by the algorithm). This complementary analysis served to assess whether findings were independent of synthetic data generation.

We evaluated 11 classification algorithms: Random Forest Classifier, K-Nearest Neighbors, AdaBoost, Gaussian Process Classifier, Multi-Layer Perceptron (Neural Network), Decision Tree, Radial Basis Function (RBF) Support Vector Machine, Logistic Regression, Linear Support Vector Machine, Quadratic Discriminant Analysis, and Gaussian Naive Bayes. All models were evaluated using the metrics mentioned above (balanced accuracy, weighted precision, weighted recall, and weighted F1 score).

For the top-performing models with distinctly different architectures (Random Forest, Multi-Layer Perceptron,

Logistic Regression and K-Nearest Neighbors), we performed hyperparameter tuning to optimize model configurations. To assess the contribution of each Aβ peptide to classification performance, we employed permutation feature importance analysis. Features causing larger decreases in accuracy are considered more important. The analysis was performed independently for each top-performing model to evaluate consistency across different algorithms.

Results

Assessing global γ-secretase activity in relation to SP phenotype

To investigate potential associations between γ-secretase (PSEN1) activity and SP presentation, we integrated and harmonized data from three recent studies [4–6], resulting in a dataset comprising 169 PSEN1 variants. We excluded six variants (D40del, E69D, V82L, V94M, T147P and A164V) due to their lack of impact on γ-secretase processivity, and hence uncertain pathogenicity. In addition, three variants (R278I, C410Y and P433S) were excluded due to their profound inhibitory impact on γ-secretase activity [5, 15]. The resulting dataset of 160 PSEN1 variants was categorized into two disease groups: 118 associated with AD without SP, and 39 associated with AD and spasticity/SP (labelled as AD and AD + SP, respectively). WT, R35Q and E318G PSEN1 served as controls (Fig. 1A, Supplementary Table 1 and -additional file 1).

To analyse the relationship between global γ-secretase activity and the SP phenotype, we compared total, secreted Aβ peptide levels between the two disease groups (Fig. 1B). Given the significant impact of experimental settings on absolute Aβ levels (pg/ml), we used for this specific analysis the largest dataset reporting pg/ml values [4], and applied the same filtering criteria as in the integrated data. This resulted in a dataset with 96 AD and 27 AD + SP PSEN1 variants. We used the sum of Aβ37, 38, 40, 42 and 43 peptides as a proxy for global γ-secretase activity. The mean total Aβ levels were comparable between AD (mean ± SD: 18035 ± 8698 pg/ml) and AD + SP (mean ± SD: 19227 ± 9491 pg/ml) groups ($p = 0.67$). Notably, we found no significant difference in the total Aβ levels between the groups, suggesting that

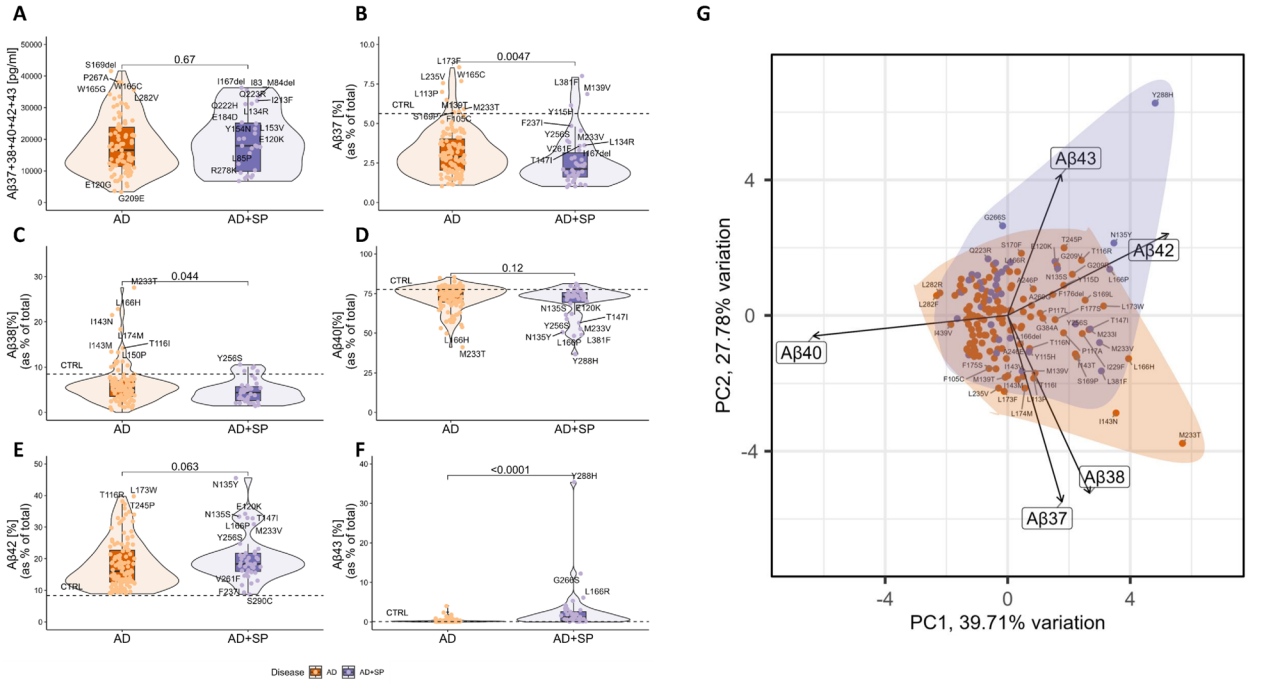

Fig. 1 Relationship between Aβ profiles and ADAD phenotypic presentation. **A** Schematic representation of PSEN1 primary structure highlighting residues affected by selected mutations studied in this report. Color-coding of mutations: green (benign, control), orange (AD ($n = 118$)), purple (AD + SP ($n = 39$)), double color orange and purple (mutations in that residue associated with AD and with AD + SP). PSEN1 catalytic aspartic acids are shown in pink. Pathogenicity information taken from the Alzforum database. **B** Total Aβ peptide levels (sum of Aβ37, 38, 40, 42 and 43) compared between AD ($n = 96$) and AD + SP ($n = 27$) groups. Box plots show median, first and third quartiles, and 1.5 inter-quartile range (IQR). Individual points represent individual PSEN1 variants. Values are expressed as pg/ml. Statistics were calculated using Wilcoxon Signed Rank Test. **C-G** Relative levels of (**C**) Aβ37, (**D**) Aβ38, (**E**) Aβ40, (**F**) Aβ42 and (**G**) Aβ43 levels expressed as the percentage of total Aβ and compared between AD and AD + SP groups. Box plots show median, first and third quartiles, and 1.5 inter-quartile range (IQR). Statistics were calculated using Wilcoxon Signed Rank Test. **H** The PCA of Aβ profiles showing the distribution of AD ($n = 118$) and AD + SP ($n = 39$) variants in the PC1-PC2 space. Loading vectors indicate the contribution of each Aβ peptide to the principal components. Percentage of variance explained by each component is indicated on the axes. The PCA points to the association between high Aβ43 levels and SP

the SP phenotype is not associated with alterations in the global γ-secretase activity, at least when using APP as a substrate.

Differential impairments of γ-secretase processivity and product-line preference in AD and AD+SP groups

To further characterize the relationship between Aβ profiles and the SP phenotype, we analysed the relative amounts of individual Aβ37, 38, 40, 42 and 43 peptides (as percentage of total Aβ (Aβ profiles)) using an integrated dataset from three recent studies [4–6]. We cross-normalised the data using the WT PSEN1 Aβ profile as an internal reference. Our analysis revealed that the AD + SP group exhibited significantly higher Aβ43 levels and lower amounts of Aβ37 and Aβ38, compared to the AD group (Fig. 1C-G). Principal component analysis (PCA), which enables visualization of complex data in a two-dimensional space, corroborated that SP-linked PSEN1 mutations are characterised by Aβ profiles enriched in Aβ43 peptides (Fig. 1H, additional file 2). Since the PSEN1 Y288H variant was associated with very high levels of Aβ43, to ensure that the conclusions are not driven by only one mutant, we re-analysed the data upon its exclusion (Additional file 3). All the conclusions, but the significance of the Aβ38 change, remained valid upon its exclusion.

Given the association between reduced γ-secretase processivity (assessed by the Aβ37 + 38 + 40/42 + 43 ratio) with earlier dementia onset and faster deterioration in biomarker measures across PSEN1 variants [4–6], we examined whether PSEN1 mutations leading to more pronounced impairments in the processivity of the enzyme are enriched in the AD + SP group. We found a significantly more profound reduction in the enzyme processivity among mutations linked to SP, relative to those associated with pure dementia phenotype (Fig. 2A). We also evaluated whether changes in the product-line preference of γ-secretase, leading to increased production of either Aβ42 and Aβ38 or Aβ43, Aβ40 and Aβ37 peptides, could differentiate SP-linked PSEN1 mutations. Notably and regardless of the group, the vast majority of the PSEN1 mutations shifted the Aβ production in favour of Aβ38 and Aβ42, relative to the control variants (dotted line in Fig. 2B). We found however, no significant difference between the AD and AD + SP groups.

To further explore mutation-induced alterations in γ-secretase function, we analysed the relationship between γ-secretase processivity and product-line preference. We found linear relationships with similar slopes, but significant differences in Y-intercepts ($P = 0.0013$) between the AD and AD + SP groups. The similar slopes (~ 0.5) indicate an association between γ-secretase processivity and product-line preference: the greater the mutation-induced impairment in processivity, the higher the preference for the Aβ42 generating product-line. Notably, the differences in Y-intercepts suggest that AD + SP-linked mutations exert an additional, independent effect on γ-secretase function. Specifically, at equivalent levels of processivity impairments, AD + SP group show milder shifts in the product-line preference towards the Aβ42 product-line, relative to the AD group (Fig. 2C). We further visualized this relationship on the Aβ43 vs Aβ42 plot, which clearly illustrates the distinction between the two groups (Fig. 2D).

Machine learning reveals high Aβ43 significance for SP classification

To further investigate the relationship between Aβ profiles and the disease phenotype, we employed supervised machine learning (Additional file 1). We tested 11 commonly used classifiers for their potential to classify the disease phenotype based on Aβ profiles. For this analysis, we used as a training set the integrated datasets from Liu et al. [4] and Petit et al. [5], and as a test dataset the Schultz et al. [6] dataset, ensuring independent datasets for training and testing. We implemented two complementary approaches to address class imbalance. First, we applied the SMOTE algorithm [21] and utilized the Aβ37, Aβ38, Aβ40, Aβ42 and Aβ43 levels (% as in profiles) as features to classify the variants into either AD or AD + SP classes. Second, to avoid creating synthetic data points, we analysed the data without oversampling while still accounting for class imbalance during model training. With oversampling nearly all tested models performed the classification task well, with the weighted F1 scores ranging from 0.164 to 0.91 (mean = 0.7) (Fig. 3A). This good performance indicates an association between the Aβ peptides and the disease phenotype. We then focused on the top-performing models with markedly different architectures: Random Forest Classifier (an ensemble method constructing multiple decision trees), Multi-Layer Perceptron Classifier (MLP, a deep learning neural network model), Logistic Regression (a statistical model using a logistic function) and K-Nearest Neighbours classifier [22]. After performing hyperparameter tuning on these selected models, we employed permutation feature importance analysis to estimate the contribution of each feature to the models' performance (Fig. 3B). The consistent identification of Aβ43 as the key discriminating feature across all models (Fig. 3C), regardless of the architecture, strongly supports the robustness of this association.

To further assess these findings, without relying on synthetic data generation (SMOTE), we performed an identical analysis without oversampling, accounting for class imbalance during model training. Here, the weighted F1 score ranged from 0.19 to 0.91 (mean = 0.7) (Additional file 5). Out of 11 tested architectures,

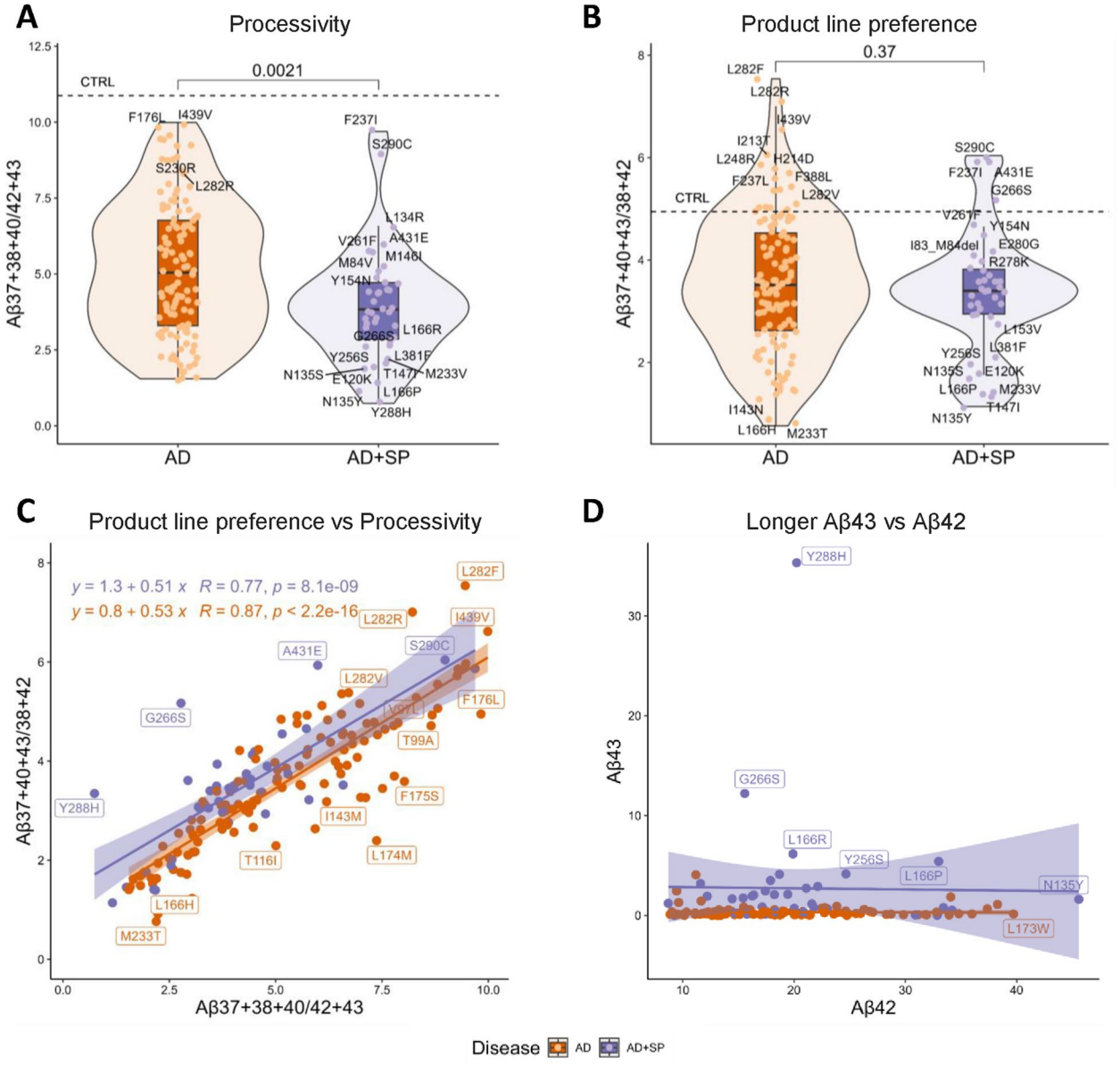

Fig. 2 Relationships between product-line preference and processivity in the context of phenotypic presentation of the disease. **A, B** (**A**)γ-secretase processivity calculated as Aβ37+38+40/42+43 and (**B**) γ-secretase product-line preference calculated as Aβ37+40+43/38+42 were compared between AD (*n*=118) and AD+SP (*n*=39) groups. Dotted line indicates mean control value. Box plots show median, quartiles, and range. Statistics were calculated using Wilcoxon Signed Rank Test. **C**, **D** Scatter plots showing the relationships between γ-secretase processivity and product-line preference for the AD and AD+SP groups, as well as between Aβ42 and Aβ43, respectively. (**C**) Linear relationships are described by the following equations: y = 0.53 x + 0.8, R^2 = 0.75, and y = 0.51 x + 1.3, R^2 = 0.60, for the AD and the AD+SP groups, respectively. Differences in the slopes are not significant (P = 0.73, F = 0.1197; DFn = 1, DFd=153); 95%CI: AD: 0.47–0.59.47.59 and AD+SP: 0.37–0.64.37.64), but differences in the Y-intercepts are significant (*P* = 0.0013; F = 10.73, DFn = 1, DFd=154) (95%CI: AD: 0.49–1.12.49.12 and AD+SP: 0.73- 1.94)

Gaussian Naive Bayes and Quadratic Discriminant Analysis, with weighted F1 scores below 0.5, were the least suitable classifiers for this task without oversampling, which is consistent with the SMOTE-based approach. For direct comparison between approaches, we focused on the same (selected above) models, performed hyperparameter tuning and conducted permutation feature importance analysis. Aβ43 was again identified as the most important feature across all evaluated models, demonstrating that this finding is independent of the class imbalance correction method.

Discussion

We conducted a comprehensive analysis of ADAD-linked Aβ profiles generated by *PSEN1* variants associated with both AD and AD + SP to investigate possible relationships

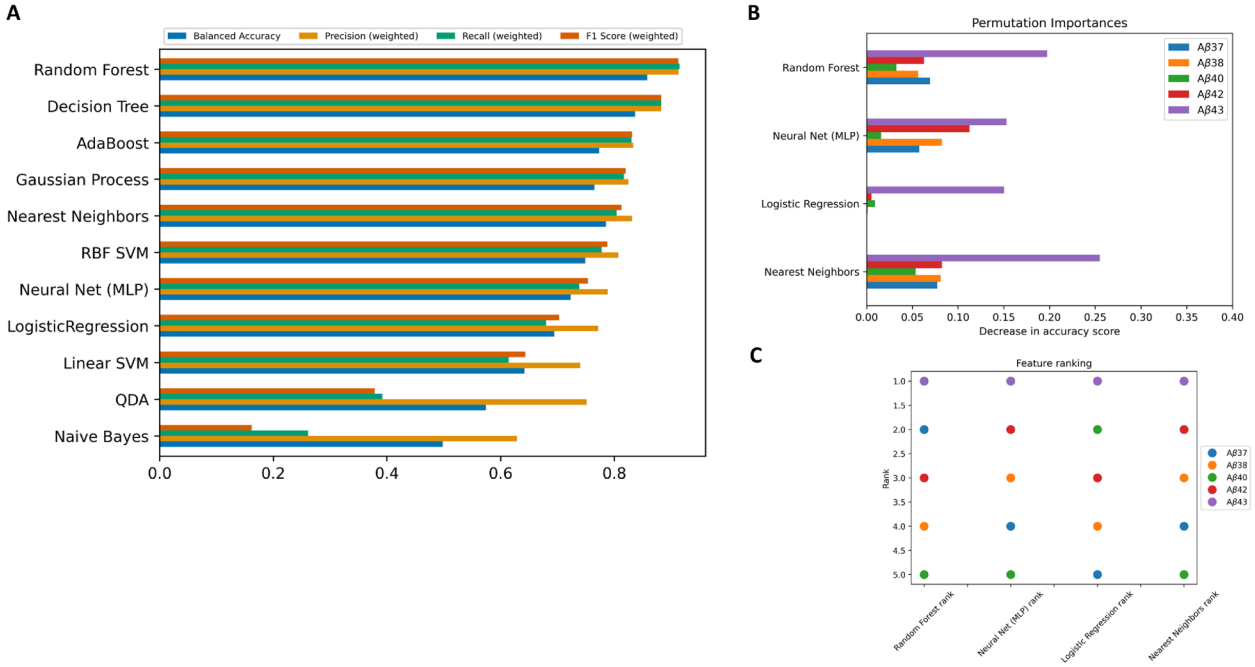

Fig. 3 Machine learning classification of AD phenotypes based on Aβ profiles. **A** Performance metrics for 11 different machine learning classifiers trained to classify AD versus AD + SP phenotypes based on Aβ profiles. Models were trained on integrated data from Liu et al. [4] and Petit et al. [5] and validated on the independent test data from Schultz et al. [6]. These data demonstrate very good performance of the classifiers to define the disease phenotype based on the Aβ profiles. **B**, **C** Feature importance analysis showing the relative contribution of each Aβ peptide to phenotype classification. (**B**) Permutation feature importance scores, and (**C**) feature ranking consistency for the top three performing models. These data point at Aβ43 as the most important feature allowing for the phenotypic disease classification

between alterations in Aβ production and the SP phenotype in carriers of *PSEN1* mutations. Our analysis integrated data from MEF and HEK293 cells. Normalization to wild-type PSEN1 within each system and the use of relative Aβ profiles (percentages) controlled for cell-type-specific differences, isolating mutation-specific effects on γ-secretase function. The analysis of total Aβ production showed no significant differences between AD and AD + SP groups, suggesting that mutation-induced alterations in the overall γ-secretase activity may not influence SP development. However, this finding warrants cautious interpretation, as total Aβ peptide amounts highly depend on cellular density as well as expression levels of both substrate and enzyme, which were not entirely controlled in any of the experimental set-ups used [4–6]. In contrast, observations regarding γ-secretase processivity can be considered more reliable, as the use of Aβ ratios or profiles normalizes for any differences in cellular density or protein expression levels.

Indeed, the magnitude of impairment in γ-secretase processivity, measured by the Aβ 37 + 38 + 40/42 + 43 ratio, was significantly greater in the AD + SP group. This finding aligns well with previous observations linking more severe processivity impairments to earlier age at dementia onset (AAO) and a higher prevalence of non-cognitive symptoms, including spasticity [11]. Our analysis of the relationship between processivity and product-line preference revealed parallel slopes but significantly different intercepts between the two groups. The parallel slopes indicate that processivity and product-line preference are coupled through a shared biochemical mechanism in both mutation classes. However, the significant intercept difference ($P = 0.0013$) indicates that AD + SP mutations are not simply more severe versions of AD mutations, but rather involve qualitatively distinct alterations in enzyme function. While AD + SP mutations cause more severe processivity defects, they induce milder shifts in product-line preference towards the Aβ42 pathway compared to pure AD mutations at matched processivity levels. The differential effect possibly involves alterations in the initial recognition of the substrate. We employed supervised machine learning to classify PSEN1 variants into AD and AD + SP phenotypes based on their Aβ profiles. Feature importance was assessed to identify the most influential Aβs in the phenotype classification. This approach further supported the association between Aβ profiles and the disease phenotype, consistently identifying Aβ43 relative levels as the most important feature for the phenotypic classification. These findings are particularly intriguing given the high amyloidogenicity and neurotoxicity of Aβ43 [15, 23, 24]. The increased Aβ43 production in the AD + SP group can be attributed to a milder mutation-induced shift from the predominant Aβ40 product-line towards

the Aβ42 line, which is seen in most pathogenic PSEN1 variants. As a result, the impairments in γ-secretase processivity particularly affect the Aβ40 product-line, providing a biochemical basis for the relative increases in Aβ43 in the SP + AD group. Our analysis however reveals a more complex association between SP and γ-secretase dysfunction: AD + SP-linked mutations have more profound detrimental effects on γ-secretase processivity, but induce milder shifts in the product-line preference towards Aβ42 generation, compared to pure AD-linked ones. This likely explains the relatively higher Aβ43 generation. These differential effects suggest specific structural impacts on γ-secretase: while both mutation types destabilize enzyme–substrate interactions, the AD variants preferentially affect the position of the first cleavage to favour the Aβ42 product-line, possibly via altered positioning of the initial APP (C99) substrate. The preferential association of SP with elevated Aβ43 rather than Aβ42 levels also suggests that distinct pathogenic mechanisms may underlie cognitive versus motor symptoms in ADAD. This could reflect either differential vulnerability of motor neurons to specific Aβ species, distinct patterns of Aβ accumulation in motor versus cognitive circuits, or both.

The precise mechanism by which distinct Aβ peptides contribute to the formation of toxic Aβ assemblies remains elusive. However, the linear correlation between the long-to-short Aβ37 + 38 + 40/42 + 43 peptide ratios (rather than absolute peptide levels) and ADAD clinical onset suggests that the balance between amyloidogenic and less amyloidogenic, more soluble peptides is critical in pathogenesis. Our findings point to a scenario where specific imbalances in Aβ profiles contribute to ADAD clinical heterogeneity, specifically, Aβ43-rich profiles to the development of SP. It is noteworthy that the SP phenotype is rarely observed in carriers of pathogenic *PSEN2* and *APP* variants, and that pathogenic mutations in those genes are typically associated with increased Aβ42 rather than Aβ43 levels [14]. While this observation and the increased Aβ43 levels measured in post-mortem brain tissue as well as iPSC-derived neurons from carriers of some PSEN1 mutations associated with atypical presentations (including SP) support the potential involvement of Aβ43 in SP development [25, 26], we acknowledge that our analysis establishes a correlative rather than a causative link. Further investigations are necessary to definitively prove or refute this relationship. Moreover, it is important to consider that the elevated Aβ43 levels associated with SP-linked PSEN1 variants may serve as a proxy for broader alterations in γ-secretase function. These alterations could potentially affect other γ-secretase substrates that could be directly involved in the development of SP, a possibility that warrants additional research.

Some studies report the presence of Aβ plaques with specific morphology (cotton-wool plaques) in post-mortem brain samples of mutation carriers affected by SP [27–30]. However, others suggest a disconnection between Aβ accumulation and SP based on brain imaging data [13, 31]. The notion that altered Aβ composition in amyloid plaques plays a role in AD aetiology is supported by the evaluation of amyloid plaque composition in post-mortem brains of AD patients and amyloid-positive, non-demented individuals [22]. The latter showed that plaques differing in their Aβ peptide composition as well as lipid content distinguish post-mortem brain samples between AD and amyloid-positive, non-demented individuals. The uncovered robust link between the altered Aβ profiles and the SP phenotype prompts a re-evaluation of the role of specific Aβ species in the heterogeneous clinical presentation of AD.

A more nuanced understanding of how altered γ-secretase function contributes to various aspects of AD pathology could lead to the development of more refined animal models that better recapitulate the observed extra-phenotypes, including the motor deficits, support the discovery of new biomarkers allowing for the phenotypic classification of the disease as well as inform the development of more personalized treatment approaches for ADAD patients. In this context, it is plausible that the re-emerging γ-secretase targeting strategies, particularly γ-secretase modulators stabilizing γ-secretase-substrate interactions [9] to normalize the processing of APP/Aβ (and potentially other substrates) or immunotherapies targeting Aβ43 could alleviate not only cognitive impairments but also the motor symptoms. If effective, those therapeutic approaches might be particularly beneficial for mutations that are associated with marked physical disability from SP at the stages when cognitive symptoms are relatively mild.

Conclusions

In conclusion, our analysis provides evidence for a correlative association between elevated Aβ43 levels and the development of SP in carriers of PSEN1 mutations. Future studies focusing on elucidating the mechanisms leading to motor symptoms in ADAD should consider this possible pathogenic link.

Limitations

It is important to note that the uncovered association between Aβ43 and the SP phenotype, while robust across multiple analytical approaches, establishes correlation rather than causation. Despite integrating the data from multiple studies, the sample size was relatively small, particularly for the AD + SP group. Due to the limited dataset, our machine learning approach may be subject to overfitting. Our analysis relies on data generated in vitro,

using cellular models that do not fully recapitulate the complexity of Aβ processing, clearance and accumulation in the human brain. Despite these constraints, the consistent identification of Aβ43 as a key discriminating feature between AD and AD + SP groups provides a strong foundation for future mechanistic studies. In addition, while we focused on Aβ profiles, other factors such as genetic and/or environmental influences, as well as additional γ-secretase substrates, may contribute to the development of the SP phenotype. These limitations underscore the need for further research, including in vivo studies and longitudinal clinical observations, to elucidate the mechanisms underlying SP development in ADAD.

Abbreviations

AAO	Age at disease onset
AD	Alzheimer's disease
ADAD	Autosomal dominant Alzheimer's disease
ANCOVA	Analysis of Covariance
APP	Amyloid precursor protein
Aβ	Amyloid beta
CLR	Centered Log-Ratio
HEK	Human embryonic kidney
iPSC	Induced pluripotent stem cells
IQR	Inter-Quartile Range
MEF	Mouse embryonic fibroblasts
MLP	Multi-Layer Perceptron
MSD-ELISA	Meso Scale Discovery Enzyme-Linked Immunosorbent Assay
PCA	Principal component analysis
PSEN1	Presenilin 1
PSEN2	Presenilin 2
RBF	Radial Basis Function
SAD	Sporadic Alzheimer's disease
SMOTE	Synthetic Minority Over-sampling TEchnique
SP	Spastic paraparesis
WT	Wild type

Supplementary Information

The online version contains supplementary material available at https://doi.org/10.1186/s13195-025-01896-3.

Additional file 1. Data analysis workflow: The scheme presents the processing of the data, i.e. intra- and inter-assay harmonisation, filtering and further univariate or supervised machine learning analysis.

Additional file 2. Principal Component Analysis (PCA): additional information regarding the PCA presented in the Figure 1. Top: Component loadings showing each Aβ peptide's contribution to PC1-PC5. Circle colour indicates loading direction (yellow: negative, blue: positive) and size indicates magnitude. Bottom left: Pairwise PC scatter plots with AD (orange) and AD+SP (blue) variants. Percentages indicate variance explained by each component. Bottom right: SCREE plot showing cumulative variance explained. The first three components (PC1: 39.71%, PC2: 27.78%, PC3: 18.64%) capture 86.13% of total variance.

Additional file 3. Re-analysis of the AD and AD+SP groups upon exclusion of the PSEN1 Y288H variant: Univariate analysis presented in Figures 1 & 2 was re-done upon the exclusion of Y288H variant, as this variant was associated with extremely high Aβ43 levels. To facilitate comparison, the results are presented using similar formatting as in Figures 1 and 2.

Additional file 4. Performance evaluation of top-performing machine learning classifiers: ROC curves (left) and Precision-Recall curves (right) for classification of PSEN1 variants into AD or AD+SP phenotypes based on Aβ profiles, evaluated on the independent test set (Schultz et al. dataset) using synthetic oversampling (SMOTE). (A) Random Forest (AUC = 0.93, AP = 0.85). (B) Neural Network (Multi-Layer Perceptron) (AUC = 0.78, AP = 0.74). (C) Logistic Regression (AUC = 0.78, AP = 0.62). (D) K-Nearest Neighbors' algorithm (AUC = 0.93, AP = 0.88). Dashed line represents random classifier performance. AUC, Area Under the Curve; AP, Average Precision.

Additional file 5. Classification performance without synthetic oversampling (SMOTE). Machine learning analysis without SMOTE, accounting for class imbalance during training. (A) Performance metrics for all 11 ML classifiers on the independent test set. (B) Permutation feature importance scores show Aβ43 as the most important feature across top-performing models. (C) Feature ranking consistency across models, with Aβ43 consistently ranked highest. (D-G) ROC and Precision-Recall curves for (D) Random Forest (AUC = 0.90, AP = 0.86), (E) Neural Network (AUC = 0.81, AP = 0.73), (F) Logistic Regression (AUC = 0.77, AP= 0.58) and (G) K-Nearest Neighbors' algorithms (AUC = 0.95, AP = 0.90). Dashed line represents random classifier performance. AUC, Area Under the Curve; AP, Average Precision.

Additional file 6: Supplementary table 1. Summary of the PSEN1 variants included in the study, associated Aβ profiles and clinical phenotypes.

Acknowledgements
We are grateful to Dr. Sara Gutiérrez-Fernández and Dr. Diego Cabezudo for their critical review of the manuscript.

Authors' contributions
KMZ: conceptualization, methodology, formal analysis, investigation, writing – original draft, funding acquisition; JB: data analysis, writing review & editing during manuscript revision; MBH: data analysis and writing review & editing during manuscript revision; TE: input on analysis, writing – review & editing; CH: input on analysis, funding acquisition, writing – review & editing; NSR: data curation, funding acquisition, writing – review & editing; LCG: conceptualization, writing – original draft, supervision, funding acquisition.

Funding
We acknowledge Stichting Alzheimer Onderzoek (Project number: 20220007 to KMZ), the Fonds Wetenschappelijk Onderzoek (FWO) (G008023N to LCG) and VIB (to LCG). NSR acknowledges support from the UK Dementia Research Institute at UCL through UK DRI Ltd, principally funded by the UK Medical Research Council, the UK NIHR UCLH Biomedical Research Centre and the Dominantly Inherited Alzheimer Network (DIAN), funded by the National Institute on Aging. CH acknowledges support from the Deutsche Forschungsgemeinschaft (DFG), grant INST874/9–1.

Data availability
All data generated or analysed during this study are included in this published article, its supplementary information files and three articles that provided basis for the analysis [4–6].

Declarations

Ethics approval and consent to participate
Not applicable.

Consent for publication
Not applicable.

Competing interests
KMZ, JB, MBH, TE, CH and NSR declare no competing interests. LGC is scientific founder of TRIM and reports consultancy for Roche and Astex Pharmaceuticals in the last 3 years.

Author details
[1]VIB-KU Leuven Center for Brain & Disease Research, Vlaams Instituut Voor Biotechnologie (VIB), Herestraat 49 Box 602, 3000 Leuven, Belgium
[2]Department of Neurosciences, Leuven Brain Institute, KU Leuven, Leuven, Belgium
[3]Molecular Biology Department, National Research Centre, Dokii, Cairo, Egypt
[4]Center for Mass Spectrometry and Optical Spectroscopy (CeMOS), Mannheim University of Applied Sciences, Mannheim, Germany

[5]Dementia Research Centre, Department of Neurodegenerative Disease, University College London Queen Square Institute of Neurology, London, UK
[6]UK Dementia Research Institute at UCL, London, UK

Received: 31 March 2025 / Accepted: 18 October 2025
Published online: 26 November 2025

References

1. Chávez-Gutiérrez L, Szaruga M. Mechanisms of neurodegeneration—Insights from familial Alzheimer's disease. In: Seminars in cell & developmental biology: 2020. Elsevier: 75–85.
2. Ryan NS, Nicholas JM, Weston PSJ, Liang Y, Lashley T, Guerreiro R, et al. Clinical phenotype and genetic associations in autosomal dominant familial Alzheimer's disease: a case series. Lancet Neurol. 2016;15(13):1326–35. https://doi.org/10.1016/S1474-4422(16)30193-4.
3. Takami M, Nagashima Y, Sano Y, Ishihara S, Morishima-Kawashima M, Funamoto S, et al. Gamma-Secretase: successive tripeptide and tetrapeptide release from the transmembrane domain of beta-carboxyl terminal fragment. J Neurosci. 2009;29(41):13042–52. https://doi.org/10.1523/JNEUROSCI.2362-09.2009.
4. Liu L, Lauro BM, He A, Lee H, Bhattarai S, Wolfe MS, et al. Identification of the Abeta37/42 peptide ratio in CSF as an improved Abeta biomarker for Alzheimer's disease. Alzheimers Dement. 2023;19(1):79–96. https://doi.org/10.1002/alz.12646.
5. Petit D, Fernandez SG, Zoltowska KM, Enzlein T, Ryan NS, O'Connor A, et al. Aβ profiles generated by Alzheimer's disease causing PSEN1 variants determine the pathogenicity of the mutation and predict age at disease onset. Mol Psychiatry. 2022;27(6):2821–32. https://doi.org/10.1038/s41380-022-01518-6.
6. Schultz SA, Liu L, Schultz AP, Fitzpatrick CD, Levin R, Bellier JP, et al. γ-Secretase activity, clinical features, and biomarkers of autosomal dominant Alzheimer's disease: cross-sectional and longitudinal analysis of the Dominantly Inherited Alzheimer Network observational study (DIAN-OBS). Lancet Neurol. 2024;23(9):913–24. https://doi.org/10.1016/S1474-4422(24)00236-9.
7. Chavez-Gutierrez L, Bammens L, Benilova I, Vandersteen A, Benurwar M, Borgers M, et al. The mechanism of gamma-Secretase dysfunction in familial Alzheimer disease. EMBO J. 2012;31(10):2261–74. https://doi.org/10.1038/emboj.2012.79.
8. Szaruga M, Veugelen S, Benurwar M, Lismont S, Sepulveda-Falla D, Lleo A, et al. Qualitative changes in human gamma-secretase underlie familial Alzheimer's disease. J Exp Med. 2015;212(12):2003–13. https://doi.org/10.1084/jem.20150892.
9. Szaruga M, Munteanu B, Lismont S, Veugelen S, Horré K, Mercken M, et al. Alzheimer's-causing mutations Shift Aβ length by destabilizing γ-Secretase-Aβn interactions. Cell. 2017;170(3):443–56. https://doi.org/10.1016/j.cell.2017.07.004.
10. Shea YF, Chu LW, Chan AO, Ha J, Li Y, Song YQ. A systematic review of familial Alzheimer's disease: differences in presentation of clinical features among three mutated genes and potential ethnic differences. J Formos Med Assoc. 2016;115(2):67–75. https://doi.org/10.1016/j.jfma.2015.08.004.
11. Tang M, Ryman DC, McDade E, Jasielec MS, Buckles VD, Cairns NJ, et al. Neurological manifestations of autosomal dominant familial Alzheimer's disease: a comparison of the published literature with the Dominantly Inherited Alzheimer Network observational study (DIAN-OBS). Lancet Neurol. 2016;15(13):1317–25. https://doi.org/10.1016/S1474-4422(16)30229-0.
12. Chelban V, Breza M, Szaruga M, Vandrovcova J, Murphy D, Lee CJ, et al. Spastic paraplegia preceding PSEN1-related familial Alzheimer's disease. Alzheimer's & Dementia: Diagnosis, Assessment & Disease Monitoring. 2021;13(1):e12186. https://doi.org/10.1002/dad2.12186.
13. Vazquez-Costa JF, Paya-Montes M, Martinez-Molina M, Jaijo T, Szymanski J, Mazon M, et al. Presenilin-1 mutations are a cause of primary lateral sclerosis-like syndrome. Front Mol Neurosci. 2021;14:721047. https://doi.org/10.3389/fnmol.2021.721047.
14. Fernandez SG, Oria CG, Petit D, Annaert W, Ringman JM, Fox NC, et al. Spectrum of γ-secretase dysfunction as a unifying predictor of ADAD age at onset across *PSEN1*, *PSEN2* and *APP* causal genes. Mol Neurodegener. 2025;20(1):48. https://doi.org/10.1186/s13024-025-00832-1.
15. Veugelen S, Saito T, Saido TC, Chavez-Gutierrez L, De Strooper B. Familial Alzheimer's disease mutations in presenilin generate amyloidogenic Abeta peptide seeds. Neuron. 2016;90(2):410–6. https://doi.org/10.1016/j.neuron.2016.03.010.
16. Raux G, Guyant-Marechal L, Martin C, Bou J, Penet C, Brice A, et al. Molecular diagnosis of autosomal dominant early onset Alzheimer's disease: an update. J Med Genet. 2005;42(10):793–5. https://doi.org/10.1136/jmg.2005.033456.
17. Labuz-Roszak B, Torbus-Paluszczak M, Becelewski J, Becelewski M, Dobrakowski P, Pierzchala K. Early onset Alzheimer's disease - a case study. Psychiatr Pol. 2021;55(2):323–30. https://doi.org/10.12740/PP/OnlineFirst/114122.
18. Miklossy J, Taddei K, Suva D, Verdile G, Fonte J, Fisher C, et al. Two novel presenilin-1 mutations (Y256S and Q222H) are associated with early-onset Alzheimer's disease. Neurobiol Aging. 2003;24(5):655–62. https://doi.org/10.1016/s0197-4580(02)00192-6.
19. Appel-Cresswell S, Guella I, Lehman A, Foti D, Farrer MJ. PSEN1 p.Met233Val in a complex neurodegenerative movement and neuropsychiatric disorder. Journal of Movement Disorders. 2018;11(1):45–8. https://doi.org/10.14802/jmd.17066.
20. Yang Y, Bagyinszky E, An SSA. Presenilin-1 (PSEN1) mutations: clinical phenotypes beyond Alzheimer's disease. Int J Mol Sci. 2023;24(9):8417. https://doi.org/10.3390/ijms24098417.
21. Chawla NV, Bowyer KW, Hall LO, Kegelmeyer WP. SMOTE: synthetic minority over-sampling technique. J Artif Intell Res. 2002;16:321–57.
22. Enzlein T, Lashley T, Sammour DA, Hopf C, Chavez-Gutierrez L. Integrative single-plaque analysis reveals signature Abeta and lipid profiles in the Alzheimer's brain. Anal Chem. 2024;96(24):9799–807. https://doi.org/10.1021/acs.analchem.3c05557.
23. Kretner B, Trambauer J, Fukumori A, Mielke J, Kuhn P-H, Kremmer E, Giese A, Lichtenthaler SF, Haass C, Arzberger T. Generation and deposition of A? 43 by the virtually inactive presenilin-1 L435F mutant contradicts the presenilin loss-of-function hypothesis of Alzheimer's disease. 2016.
24. Saito T, Suemoto T, Brouwers N, Sleegers K, Funamoto S, Mihira N, et al. Potent amyloidogenicity and pathogenicity of Abeta43. Nat Neurosci. 2011;14(8):1023–32. https://doi.org/10.1038/nn.2858.
25. Arber C, Belder CRS, Tomczuk F, Gabriele R, Buhidma Y, Farrell C, et al. The presenilin 1 mutation P436S causes familial Alzheimer's disease with elevated Abeta43 and atypical clinical manifestations. Alzheimers Dement. 2024;20(7):4717–26. https://doi.org/10.1002/alz.13904.
26. Willumsen N, Arber C, Lovejoy C, Toombs J, Alatza A, Weston PSJ, et al. The PSEN1 E280G mutation leads to increased amyloid-β43 production in induced pluripotent stem cell neurons and deposition in brain tissue. Brain Commun. 2023;5(1):fcac321. https://doi.org/10.1093/braincomms/fcac321.
27. Hardy JA, Houlden H, Baker M, McGowan E, Lewis P, Prihar G, et al. High A42 causing presenilin 1 mutations lead to the cotton wool plaques/spastic paraparesis variant of Alzheimer's disease. Neurobiol Aging. 2000;21:212.
28. Houlden H, Baker M, McGowan E, Lewis P, Hutton M, Crook R, et al. Variant Alzheimer's disease with spastic paraparesis and cotton wool plaques is caused by PS-1 mutations that lead to exceptionally high amyloid-beta concentrations. Ann Neurol. 2000;48(5):806–8.
29. Le TV, Crook R, Hardy J, Dickson DW. Cotton wool plaques in non-familial late-onset Alzheimer disease. J Neuropathol Exp Neurol. 2001;60(11):1051–61. https://doi.org/10.1093/jnen/60.11.1051.
30. Yokota O, Terada S, Ishizu H, Ujike H, Ishihara T, Namba M, et al. Variability and heterogeneity in Alzheimer's disease with cotton wool plaques: a clinicopathological study of four autopsy cases. Acta Neuropathol. 2003;106(4):348–56. https://doi.org/10.1007/s00401-003-0737-7.
31. Lyoo CH, Cho H, Choi JY, Hwang MS, Hong SK, Kim YJ, et al. Tau accumulation in primary motor cortex of variant Alzheimer's disease with spastic paraparesis. J Alzheimers Dis. 2016;51(3):671–5. https://doi.org/10.3233/JAD-151052.

Publisher's Note